Spectrochimica Acta Part A: Molecular and Biomolecular Spectroscopy 221 (2019) 117151

Contents lists available at ScienceDirect

Spectrochimica Acta Part A: Molecular and Biomolecular Spectroscopy

journal homepage: www.elsevier.com/locate/saa

Highly sensitive and straightforward methods for the detection of cyanide using profluorescent glutathionylcobalamin

Younhwa Byun [1], Safikur Rahman [1], Sungwon Hwang, Jihyun Park, Seulgi Go, Jihoe Kim *

Department of Medical Biotechnology, Yeungnam University, Gyeongsan, 712-749, South Korea

ARTICLE INFO

Article history:
Received 14 January 2019
Received in revised form 29 April 2019
Accepted 21 May 2019
Available online 23 May 2019

Keywords:
Glutathionylcobalamin
Glutathione
Cyanide
Eosin
Fluorescence
Luminescence

ABSTRACT

The extreme toxicity of cyanide and its continued use in various industries have raised concerns over environmental contamination and, therefore, considerable attention has given to develop facile and sensitive methods of cyanide detection. In this study, we developed highly sensitive and straightforward methods of cyanide detection using eosin-labeled glutathionylcobalamin (*E*-GSCbl) containing fluorescent eosin-labeled glutathione (*E*-GSH) as the upper axial ligand to the cobalt. *E*-GSH fluorescence was strongly quenched in E-GSCbl. The E-GSH ligand of *E*-GSCbl was replaced specifically by cyanide, showing recovery of the *E*-GSH fluorescence. This profluorescent property of E-GSCbl enabled detection of cyanide in aqueous solutions, yielding a lower detection limit of 10 nM (0.26 μg L^{-1}). Moreover *E*-GSH exhibited strong luminescence under UV-light that was quenched in E-GSCbl, and this allowed naked-eye detection of cyanide at concentrations as low as 100 nM. This study demonstrates that profluorescent *E*-GSCbl is a highly sensitive cyanide chemosensor that can detect nanomolar concentrations of cyanide.

1. Introduction

Cyanide is acutely toxic to humans in a dose-dependent manner at a very steep rate. Cells exposed to cyanide exhibit cellular anoxia caused by inactivation of cytochrome *c* oxidase and the inhibition of cellular respiration [1,2]. Despite its extreme toxicity, cyanide continues to be used in various industries such as gold mining, petrochemical production, metal electroplating and steel manufacture, and thus, poses a threat to the environment [3]. Moreover, a variety of species naturally produce cyanide for self-defense [4–6]. For example, agriculturally important plants such as sorghum, cassava and peaches produce cyanogenic glycosides that can release cyanide upon acid hydrolysis [7]. In addition, humans may be exposed to cyanide by inhaling smoke in fire accidents burning biomass and synthetic materials, and such cyanide exposure needs to be rapidly and accurately analyzed for emergency treatment. Due to the risks posed by potential cyanide exposure, strict regulations and guidelines have been issued regarding permissible cyanide concentrations in foods and environmental media. In particular, cyanide in drinking water must not exceed 70 μg L^{-1} (2.7 μM) ("World Health Organization, Guidelines for Drinking-Water Quality," 2008). Thus, accurate and efficient methods are essential for the detection of cyanide in environmental media. Various methods have been developed for the detection of cyanide [8]. To detect small amounts of cyanide, however, most current methods available require extensive work-up procedures as well as expensive and bulky laboratory systems [6,9].

Vitamin B_{12} (cyanocobalamin, CNCbl) was shown to be a specific chemosensor that allowed the straightforward detection of cyanide at millimolar concentrations [10]. Later, various corrin-based derivatives were developed with lower detection limits in the micromolar concentration range [11–13]. Recently, we developed methods for the detection of cyanide using a vitamin B_{12} derivative, glutathionylcobalamin (GSCbl), containing glutathione (GSH) as the upper axial ligand to cobalt in the center of the corrin ring [14]. GSCbl-based methods of cyanide detection involve the replacement of the GSH ligand by cyanide, generating cyanocobalamin (CNCbl) via dicyanocobalamin (diCNCbl) intermediate. CNCbl and diCNCbl were measured by a spectrometric assay and a naked-eye assay, respectively, for the detection of cyanide. In addition, GSH dissociated from GSCbl was conjugated with monochlorobimane, which was measured by a fluorometric assay for the detection of cyanide.

GSCbl-based methods are straightforward and highly specific for the detection of cyanide, but detection sensitivities (lower detection limits = 1.0–20 μM (26–520 μg L^{-1})) were insufficiently high to detect nanomolar concentrations of cyanide. Moreover cyanide toxicity was shown to be accumulative, when long-term exposure occurs by administration of cyanide at low concentrations [15,16]. In the present study, we developed highly sensitive and straightforward methods for the detection of cyanide using profluorescent eosin-labeled GSCbl (*E*-GSCbl)

* Corresponding author at: Department of Medical Biotechnology, Yeungnam University, Gyeongsan 712-749, South Korea.
E-mail address: kimjihoe@ynu.ac.kr (J. Kim).
[1] These authors contributed equally.

https://doi.org/10.1016/j.saa.2019.117151
1386-1425/

containing fluorescent eosin-labeled GSH (*E*-GSH) the upper axial ligand to the cobalt (Scheme 1). The fluorescence of *E*-GSH was strongly quenched in E-GSCbl. The E-GSH ligand of E-GSCbl was replaced specifically by cyanide, showing recovery of the *E*-GSH fluorescent, which enabled fluorescence turn-on detection of cyanide at nanomolar concentrations (Scheme 2). In addition, *E*-GSH exhibited strong luminescence under UV-light, which was also quenched in *E*-GSCbl, and this allowed straightforward naked-eye detection of cyanide. These results demonstrate that profluorescent E-GSCbl is a highly sensitive chemosensor that is able to detect nanomolar concentrations of cyanide.

2. Materials and methods

2.1. Materials

Chemicals of analytical grade were purchased from Sigma Aldrich, unless otherwise indicated. Potassium cyanide (KCN) solution was freshly prepared in 20 mM NaOH and neutralized before use and a cyanide standard from Sigma was used to control the quality of determination methods. Stock solutions (500 mM) of Cl^-, F^-, Br^-, I^-, SCN^-, S^{2-}, SO_3^{2-}, $S_2O_3^{2-}$, HSO_3^-, NO_3^-, HCO_3^-, PO_4^{3-} or SO_4^{2-} were prepared by dissolving proper amounts of sodium salts in distilled and deionized water.

2.2. Synthesis of eosin-labeled glutathione and glutathionylcobalamin

Eosin-labeled glutathione disulfide (Di-*E*-GSSG) was prepared, as described previously [17], and concentrations of Di-*E*-GSSG were determined by using the extinction coefficient of ε523 nm = 112 mM^{-1} cm^{-1}. Eosin-labeled glutathione (*E*-GSH) was prepared by reducing Di-E-GSSG with 40-fold molar excess dithiothreitol (DTT). E-GSH was precipitated by adding 10-volume of ice-chilled acetonitrile (CAN) and centrifuging to remove excess DTT. *E*-GSH concentrations were determined by using an extinction coefficient of ε519 nm = 88 mM^{-1} cm^{-1} [18].

Eosin-labeled glutathionylcobalamin (*E*-GSCbl) was synthesized by following a patented method (US patent number 7,030,105) with some modifications, as previously described [19]. Briefly, aquacobalamin (OH_2Cbl) was mixed with *E*-GSH at a molar ratio of 1:1.5 and the generation of *E*-GSCbl was followed by recording changes in the absorption spectrum. After incubation for 2 h in the dark at room temperature, *E*-GSCbl was precipitated by adding 10-volume of ice-chilled ACN and excess E-GSH was removed by centrifugation. E-GSCbl precipitates were dissolved in appropriate buffer and *E*-GSCbl concentrations were determined by using the extinction coefficient of ε372 nm = 14 mM^{-1} cm^{-1} [20].

2.3. HPLC analysis

Cobalamins were analyzed by HPLC as previously described [21]. A reaction mixture contained 50 μM E-GSCbl and 200 μM KCN in 50 mM Tris/HCl pH 7.5. After 2 h incubation in the dark at room temperature, the reaction mixture was loaded on an ODS-3 V C_{18} reversed phase column (250 × 4.6 mm, 5 μm, GL Sciences) equilibrated with solvent A (0.1% (*v*/v) trifluoroacetic acid/H_2O). The column was then washed with solvent A for 5 min and eluted with a linear gradient from 0 to 40% solvent B (0.1% (v/v) trifluoroacetic acid/acetonitrile) over 40 min at a flow rate of 1 mL min^{-1}, eluent was monitored at 255 nm. Standard cobalamins OH_2Cbl, CNCbl and *E*-GSCbl were eluted at retention times of 17.9 min, 21.2 min and 23.0 min, respectively. The retention time of the cobalamin product obtained in the reaction of *E*-GSCbl with KCN was compared with the retention times of standard cobalamins.

E-GSH released from E-GSCbl by cyanide replacement was identified by HPLC analysis with some modifications [19,21]. Briefly, reaction mixtures contained 50 μM E-GSCbl and 200 μM KCN (5200 μg L^{-1}) in 50 mM Tris/HCl pH 7.5. After 2 h incubation in the dark at room temperature, reaction mixtures amino groups of glutathione were derivatised with 2,3-dinitrofluorobenzene flowing the reaction of free thiols with monoiodoacetic acid and injected on a on a Bondclone NH_2 column (300 mm × 3.9 mm, 10 μm, Phenomenex) equilibrated with solvent C (80% (*v*/v) methanol/water). The column was washed with 60% solvent D (a mixture of 400 mL of solvent A with a 100 mL solution of 272 g sodium acetate trihydrate, 122 mL water and 373 mL glacial acetic acid) for 5 min and eluted with a gradient of 60–100% solvent D over 40 min at a flow rate of 1 mL min^{-1} with eluent monitoring at 255 nm. *E*-GSCbl and E-GSH were eluted at retention times of 11.6 min and 13.5 min, respectively. The retention time of *E*-GSH product generated in the reaction of E-GSCbl with KCN was compared with the retention time of the E-GSH standard.

2.4. Spectrophotometric assays

Spectrophotometric assays contained 10 μM E-GSCbl in 50 mM Tris/HCl pH 9.0 and initiated by the addition of the indicated concentrations of KCN. Reactions were followed under dark conditions for 2 h at room temperature by recording absorption spectra using a Cary 100 UV–Vis spectrophotometer (Varian). CNCbl generation was calculated by plotting A361 nm versus KCN concentrations by simple linear regression analysis (Δε361 nm = 14.2 mM^{-1} cm^{-1}) [14]. The detection limit of the spectrophotometric assay was determined according to IUPAC recommendation [22]: lower limit of detection = 3SD/s, SD is the standard deviation of the blank measurements ($n \geq 7$), s is the slope of the titration curve.

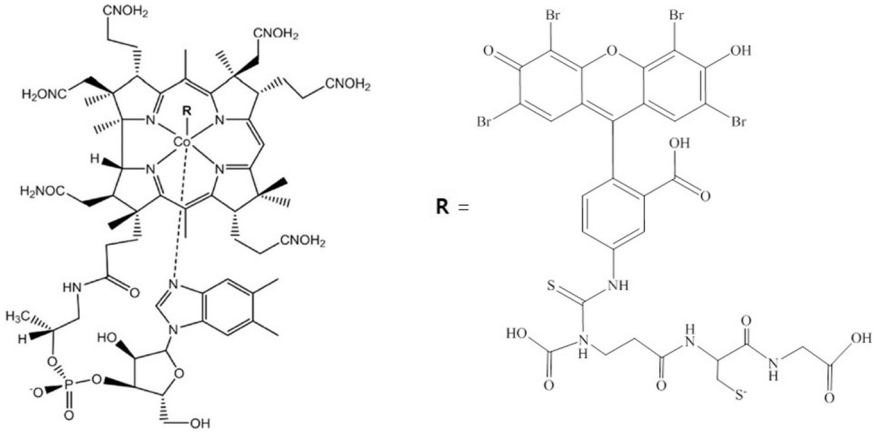

Scheme 1. Chemical structures of eosin-labeled glutathionylcobalamin and glutathione. R is the upper axial ligand and DMB (5,6-dimethylbenzimidazole) is the lower axial ligand to the cobalt in cobalamin (left). Eosin-labeled glutathionylcobalamin (*E*-GSCbl) contains eosin-labeled glutathione (E-GSH) is the upper axial ligand (right).

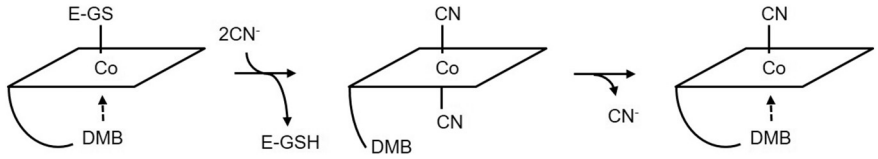

Scheme 2. Proposed mechanism for the reaction between *E*-GSCbl and cyanide. The replacement of the E-GSH ligand of E-GSCbl (left) is initiated by the nucleophilic attack of CN^-, forming the diCNCbl intermediate (middle) and generating the CNCbl product (right).

The influence of pH on the generations of diCNCbl and CNCbl was examined in the range of pH = 5.0–11.0 using different buffers (100 mM Na citrate pH 5.0, 100 mM MES pH 6.0, 100 mM Tris/HCl pH 7.0 and 8.0, 100 mM CHES pH 9.0 and 10.0, 100 mM $NaHCO_3$ pH 11.0, and 50 mM Na_2HPON_4 pH 12.0). Generation of diCNCbl and CNCbl was followed at 580 nm and 361 nm, respectively. Maximum levels of diCNCbl and CNCbl were measured by taking ΔA580 nm at 10 min (A580 nm at 10 min – A580 nm at 0 min) and ΔA361 nm at 120 min (A361 nm at 120 min – A361 nm at 0 min), respectively.

2.5. Fluorometric assays

Fluorometric assays contained 0.5 μM or 10 μM *E*-GSCbl in 50 mM Tris/HCl pH 9.0 and initiated by the addition of the indicated concentrations of KCN. After 1 h incubation in the dark at room temperature, the fluorescence of *E*-GSH released from E-GSCbl was measured at the excitation/emission wavelength of 500 nm/540 nm using a fluorescence spectrometer LS-55 (Perkin Elmer). Concentrations of E-GSH generated in reaction mixtures were determined using a standard curve obtained with synthesized E-GSH. The plot of E-GSH versus KCN concentrations was analyzed by simple linear regression analysis and the detection limit was calculated according to IUPAC recommendation [22]: lower limit of detection = 3SDb/s, SDb is the standard deviation of the blank measurements ($n \geq 7$), s is the slope of the standard curve.

2.6. Naked-eye detection under UV-light

Reaction mixtures contained 1.0 μM *E*-GSCbl and the indicated concentrations of KCN in 50 mM Tris/HCl pH 9.0. After 1 h incubation in the dark at room temperature, reaction mixtures were exposed to UV-light and luminances were recorded using a Gel Doc XR system (Bio-Rad).

3. Results

3.1. Syntheses of E-GSH and E-GSCbl

Glutathione disulfide (GSSG) was labeled with eosin (2′,4′,5′,7′-tetrabromofluorescein) at the amino groups of the glutamate residues, as previously described [17]. Eosin-labeled GSSG was reduced using dithiothreitol to produce eosin-labeled glutathione (*E*-GSH), as described in the materials and methods. Next, eosin-labeled glutathionylcobalamin (E-GSCbl) was synthesized by reacting *E*-GSH with aquocobalamin (OH_2Cbl). The addition of E-GSH to OH_2Cbl induced changes in the absorption spectrum showing the decrease at 351 nm with concomitant increases at 372 nm and 570 nm (Fig. 1A and B). Clear isosbestic points were detected at 340 nm, 365 nm and 528 nm (Fig. 1B). Subtracted spectra for the reaction of *E*-GSH with OH_2Cbl (the last spectrum – spectra obtained at different incubation times) showed absorption differences similar with those between authentic GSCbl and OH_2Cbl, except in the region around 500 nm because of interference by the strong *E*-GSH absorption (Fig. 1B and C).

3.2. Replacement of the E-GSH ligand of E-GSCbl by cyanide, generating CNCbl via diCNCbl intermediate

The reaction between E-GSCbl and cyanide was examined by UV-absorption spectroscopy (Fig. 2). The addition of KCN to *E*-GSCbl induced immediate changes in the absorption spectrum developing the absorption peak at 368 nm and a shoulder around 580 nm for a reaction intermediate (Fig. 2A and C). Further incubation produced gradual changes in the absorption spectrum of the intermediate showing a shift of the absorption peak from 368 nm to 361 nm and a concomitant absorption decrease at 580 nm (Fig. 2B and C). The difference in the absorption spectrum between *E*-GSCbl and the reaction intermediate showed peaks at 368 nm and 580 nm characteristic of diCNCbl (Fig. 2D, Sub A = intermediate – *E*-GSCbl). Moreover, the difference in the absorption spectrum between the final product and the reaction intermediate showed peaks at 361 nm and 550 nm characteristic of CNCbl (Fig. 2D, Sub B = final product - intermediate). The generation of CNCbl in the reaction of *E*-GSCbl with cyanide was confirmed by HPLC analysis (Fig. 3A). These results indicated that the upper axial ligand, E-GSH, of E-GSCbl was replaced by cyanide, generating CNCbl via diCNCbl intermediate (Scheme 2).

3.3. Induction of the replacement of the E-GSH ligand by the nucleophilic attack of cyanide anion

The reaction between E-GSCbl and KCN (molar ratio of E-GSCbl/KCN = 0.8) was examined at different pH. Generation of diCNCbl, the reaction intermediate, was followed at 580 nm. The absorption at 580 nm

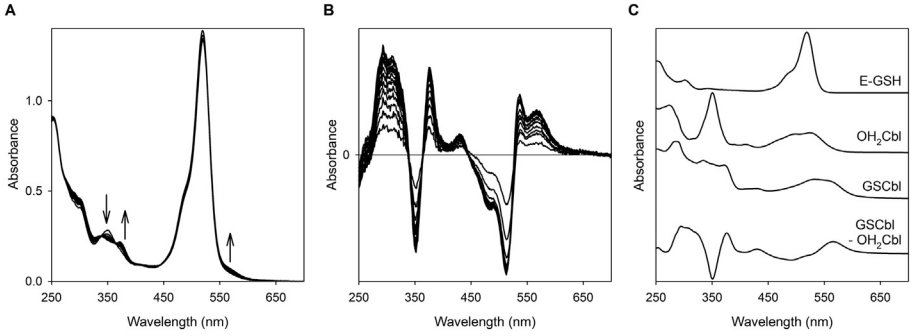

Fig. 1. Generation of *E*-GSCbl in the reaction of E-GSH with OH_2Cbl. (A), absorption spectra for the reaction of 10 μM OH_2Cbl with 15 μM eosin-labeled GSH (*E*-GSH) recorded at every 2 min of incubation. Arrows indicate the absorption decrease at 351 nm, and the increases at 372 nm and 570 nm. (B), absorption differences obtained by subtracting each spectrum from the last spectrum in A. (C), absorption spectra for *E*-GSH and the indicated standard cobalamins. The absorption difference (GSCbl - OH_2Cbl) was obtained by subtracting the spectrum of OH_2Cbl from the spectrum of GSCbl.

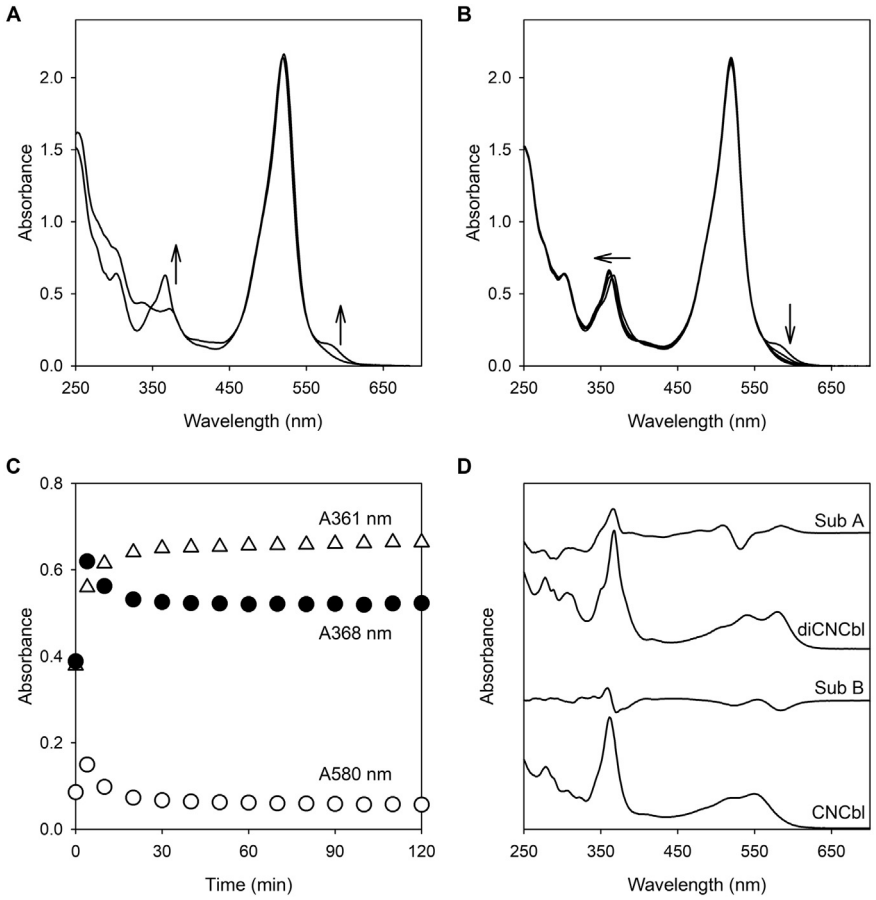

Fig. 2. Generation of CNCbl via diCNCbl intermediate in the reaction of *E*-GSCbl with cyanide. (A), absorption spectra for 25 μM E-GSCbl and immediately after the addition of 1.0 mM KCN. Arrows indicate the absorption increases at 368 nm and around 580 nm. (B), absorption spectra at every 5 min of reaction incubation after A. Arrows indicate the shift in the absorption peak from 368 nm to 361 nm and the absorption decrease around 580 nm. (C), absorption changes for the reactions in (A) and (B) at 361 nm (open triangles), 368 nm (closed circles) and 580 nm (open circles). (D), absorption spectra for the indicated cobalamins and absorption differences: Sub A = the spectrum of the reaction intermediate in (A) - the spectrum of *E*-GSCbl; Sub B = the spectrum of the product in (B) - the initial spectrum in (B).

increased for 10 min and then decreased with further incubation (Fig. 4A), indicating the rapid generation of diCNCbl and its conversion to CNCbl. The maximum levels of diCNCbl were increased in a sigmoidal-shaped curve by increasing pH (Fig. 4C). The optimum pH range for the generation of diCNCbl was pH > 9.0. In other experiments, generation of the reaction product CNCbl was followed at 361 nm for 2 h (Fig. 4B). Levels of CNCbl production were increased by increasing pH, which was plotted in a sigmoidal-shaped curve (Fig. 4D). CNCbl generation appeared to be optimized in the range of pH ≥ 8.0, but some interference occurred in the absorption at 361 nm above pH = 9.0, because of the stability of diCNCbl enhanced at high pH and its incomplete conversion to CNCbl (Fig. 4D). Considering the p*K*a of HCN/CN^- = 9.04, these results indicated that the nucleophilic attack of CN^- induces the replacement of the *E*-GSH ligand of E-GSCbl.

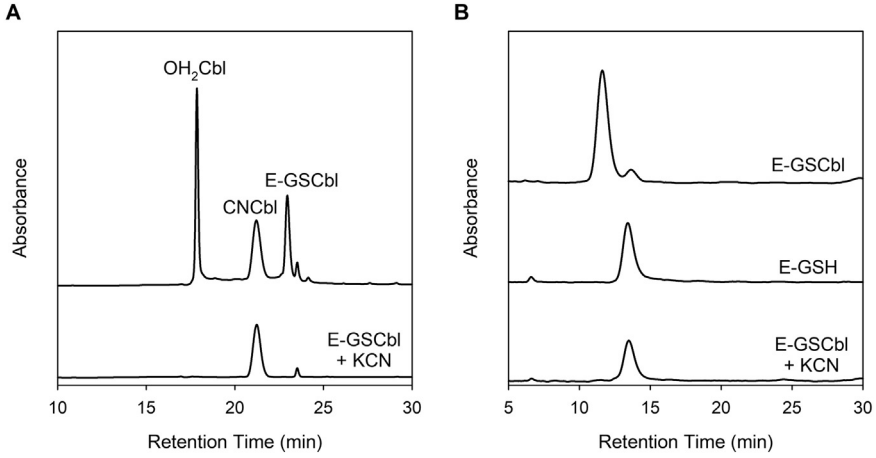

Fig. 3. HPLC analysis for products in the reaction of *E*-GSCbl with cyanide. (A), comparison of the elution profiles of the indicated standard cobalamins and the cobalamin product generated in the reaction of 25 μM E-GSCbl with 1 mM KCN. (B), comparison of the elution profiles of E-GSCbl, E-GSH and the product generated in the reaction of 25 μM E-GSCbl with 1 mM KCN.

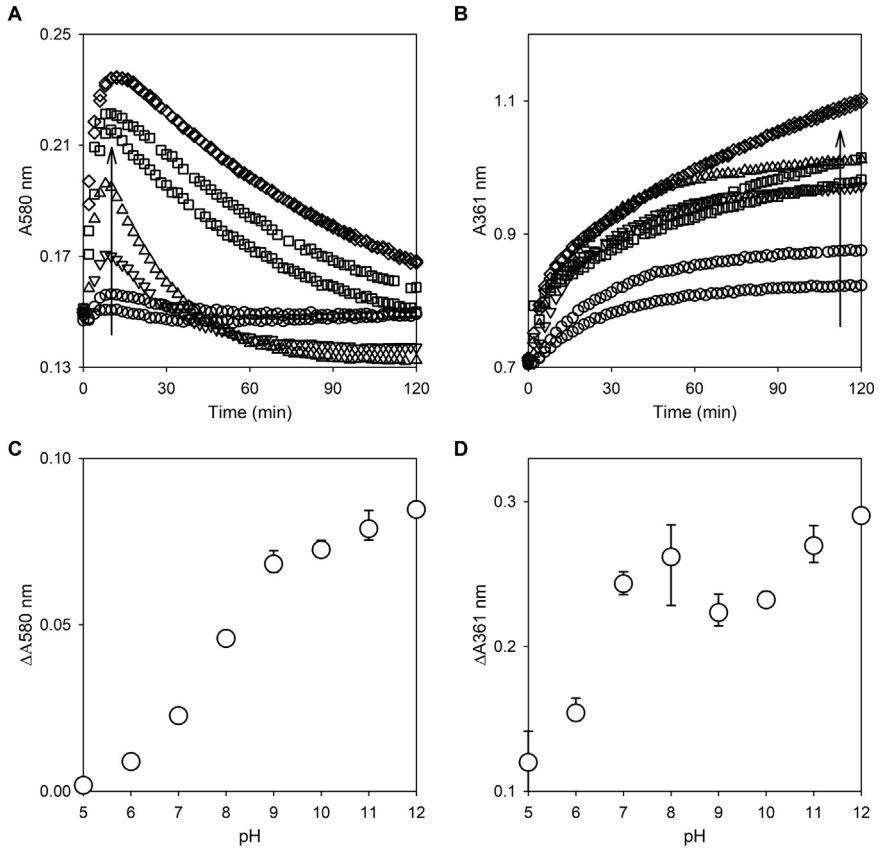

Fig. 4. Influence of pH on the reaction of E-GSCbl with cyanide. The reaction of 50 μM E-GSCbl with 40 μM KCN at pH = 5.0–12.0 was followed at 580 nm and 361 nm for the generation of diCNCbl and CNCbl, respectively. Arrows indicate the increases of A580 nm at 10 min incubation and of A361 nm at 120 min incubation by increasing pH of the reaction buffer. Levels of diCNCbl and CNCbl were plotted against pH in (C, ΔA580 nm = A580 nm at 10 min - A580 nm at 0 min) and (D, ΔA361 nm = A361 nm at 120 min - A361 nm at 0 min), respectively.

3.4. Quenching of the fluorescence of E-GSH in E-GSCbl

E-GSH exhibited strong fluorescence at 540 nm upon the excitation at 500 nm, whereas E-GSCbl exhibited little fluorescence, indicating quenching of *E*-GSH fluorescence in E-GSCbl (Fig. 5A). The reaction between *E*-GSCbl and dithiothreitol, which is known to cause reductive dissociation of the upper axial ligand of cobalamins, showed the recovery of *E*-GSH fluorescence (Fig. 5A). In addition, E-GSH fluorescence was immediately recovered upon the addition of cyanide to *E*-GSCbl and the replacement of the E-GSH ligand (Fig. 5A and B). HPLC analysis confirmed the release of E-GSH from E-GSCbl by cyanide (Fig. 3B).

3.5. Anion specificity for the replacement of the E-GSH ligand of E-GSCbl

To examine anion specificity, E-GSCbl was incubated with various anions (Br^-, SCN^-, HCO_3^-, PO_4^{3-}, Cl^-, F^-, I^-, NO_3^-, $S_2O_3^{2-}$, SO_4^{3-}, S^{2-}, SO_3^{2-}, HSO_3^-) in excess (500-fold molar equivalents). Most of the tested anions did not induce any significant change in the absorption spectrum of E-

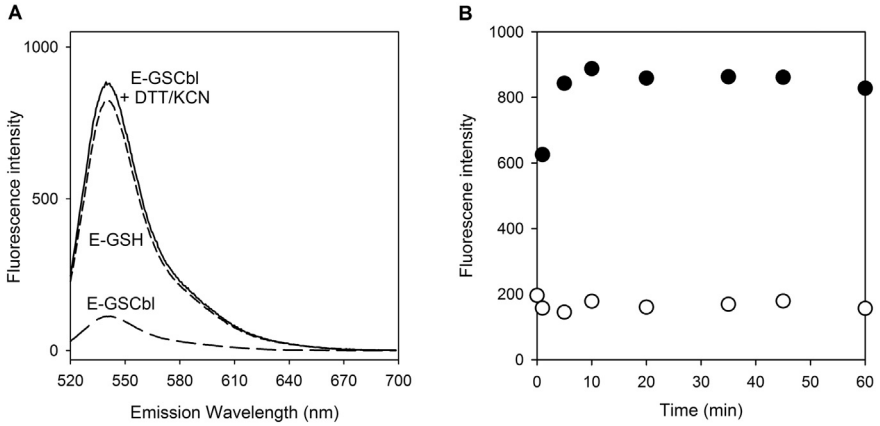

Fig. 5. Fluorescence of E-GSH and its quenching in E-GSCbl. Fluorescence spectra (A) were recorded upon the excitation at 500 nm for 1.0 μM E-GSH (short dashed line), 1.0 μM E-GSCbl (long dashed line), and 1.0 μM E-GSCbl with 0.5 mM DTT or 0.5 mM KCN (solid lines). The fluorescence (B) was followed at the excitation/emission wavelengths of 500 nm/540 nm by incubation of the reaction of 1.0 μM E-GSCbl with 0.5 mM KCN (closed circles) or without KCN (open circles).

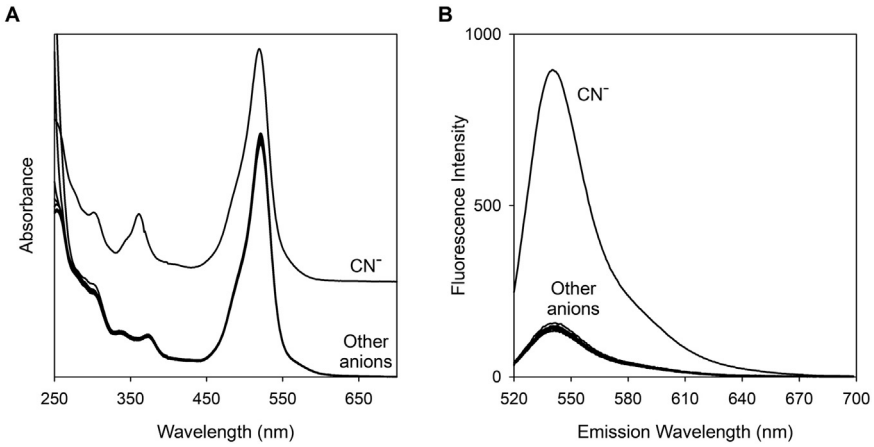

Fig. 6. Anion specificity for the reaction with E-GSCbl. (A) and (B), absorption and fluorescence spectra, respectively, for the reaction of 10 μM E-GSCbl with 100 μM CN^-, other anions (Br^-, SCN^-, HCO_3^-, PO_4^{3-}, Cl^-, F^-, I^-, NO_3^-, $S_2O_3^{2-}$, SO_4^{3-}) at 5 mM, or S^{2-}, SO_3^{2-} or HSO_3^- at 0.5 mM.

GSCbl, or in the fluorescence spectrum (Fig. 6). Incubation of E-GSCbl with S^{2-}, SO_3^{2-} or HSO_3^- at 500-fold molar equivalents produced changes in the absorption and fluorescence spectrum of *E*-GSCbl (supplementary figure), but did not at low concentrations <50-fold molar equivalents.

3.6. Spectrometric determination of cyanide

For the spectrometric determination of cyanide, *E*-GSCbl was reacted with different concentrations of cyanide and generated CNCbl was measured at 361 nm (Fig. 7A). The concentration of CNCbl increased in proportion to cyanide concentration (Fig. 7B). Analysis of a plot of [CNCbl] versus [KCN] and fitting to a first order equation resulted in a linear determination range of 0.8–10 μM (21–260 μg L^{-1}) (Fig. 7B inset). The lower detection limit was estimated to be 0.8 μM (21 μg L^{-1}), which was similar to the result obtained using GSCbl [14]. Spectrophotometric determinations of cyanide in tap water and pond water were found to have an accuracy of ≥90% (Table 1).

3.7. Fluorometric determination of cyanide

Cyanide was also determined by fluorometric assay by measuring the fluorescence of *E*-GSH fluorescence after reacting E-GSCbl with different concentrations of cyanide (Fig. 8A). The fluorescence at 520 nm increased in proportion to cyanide concentration (Fig. 8B). Analysis of a plot of [*E*-GSH] versus [cyanide] and fitting to a first order equation resulted in a linear determination range of 0.01–0.75 μM (0.26–19.5 μg L^{-1}) (Fig. 8B inset). The lower detection limit was estimated to be 0.01 μM (0.26 μg L^{-1}), which was 100-fold lower than the reported value of GSCbl-based fluorometric assay [14]. Fluorometric determinations of cyanide in tap water and pond water were found to have an accuracy of ≥95% (Table 1).

3.8. Naked-eye detection of cyanide

E-GSH was strongly luminescent under UV-light and completely quenched in *E*-GSCbl, which allowed straightforward detection of cyanide by naked-eye (Fig. 9A). The E-GSH luminance was observed after reacting E-GSCbl with cyanide. This naked-eye assay enabled detection of cyanide at concentrations as low as 0.1 μM (2.6 μg L^{-1}) in distilled water, tap water and pond water (Fig. 9B, C and D).

4. Discussion

Previously developed GSCbl-based methods are simple and highly specific for the detection of cyanide by spectrometric, fluorometric, and naked-eye assays. However these methods are not sensitive enough to detect nanomolar concentrations of cyanide. In the present study, we synthesized profluorescent eosin-labeled GSCbl (*E*-GSCbl) containing fluorescent eosin-labeled GSH (E-GSH) (Scheme 1). GSH was labeled with strongly fluorescent eosin and *E*-GSCbl was synthesized by reacting E-GSH with OH_2Cbl. The reaction of E-GSCbl synthesis showed changes in the absorption spectrum characteristic for the conversion of OH_2Cbl to E-GSCbl (Fig. 1). Characterization of synthesized E-GSCbl by

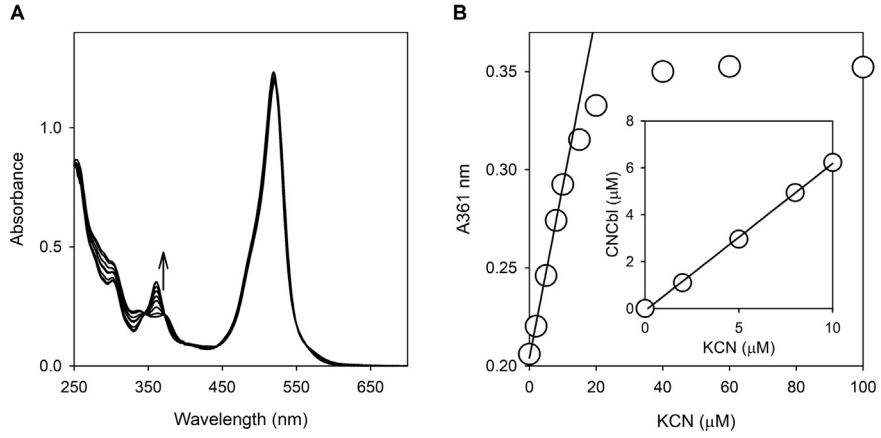

Fig. 7. E-GSCbl-based spectrometric determination of cyanide. (A), absorption spectra for the reaction of 15 μM E-GSCbl with 0–200 μM KCN. The arrow indicates the absorption increase at 361 nm by increasing cyanide concentrations. (B), plots of A361 nm versus KCN concentration and a simple linear regression analysis (solid lines in inset).

Table 1
Determination of cyanide in water samples by spectrophotometric and fluorometric assays.

Cyanide (μM)	Tap water		Pond water	
	Spectrometric (μM)	Fluorometric (μM)	Spectrometric (μM)	Fluorometric (μM)
0.25	ND	0.26 ± 0.01	ND	0.26 ± 0.03
0.50	ND	0.50 ± 0.02	ND	0.51 ± 0.02
2.00	2.2 ± 0.3	2.00 ± 0.08	2.3 ± 0.5	2.09 ± 0.09
5.00	4.9 ± 0.2	5.21 ± 0.17	5.5 ± 0.3	5.33 ± 0.21

ND: not determined, values are the means ± SD ($n \geq 10$).

the reductive dissociation of the E-GSH ligand and by cyanide replacement indicated that E-GSH formed the upper axial ligand of E-GSCbl likely via Co—S bond (Fig. 5), as demonstrated for the GSH ligand of GSCbl [23].

The *E*-GSH ligand of E-GSCbl was replaced specifically by cyanide, generating CNCbl via diCNCbl intermediate (Figs. 2 and 3) and this replacement reaction was initiated by the nucleophilic attack of CN^- (Fig. 4). These results suggest that the reaction proceeds in a manner similar to that proposed for the reaction between GSCbl and cyanide [14]. The reaction intermediate diCNCbl was generated by sequential displacement of the DMB lower axial ligand and the *E*-GSH upper axial ligand by cyanide (Scheme 2). The diCNCbl intermediate was slowly converted into CNCbl as the cyanide lower axial ligand was replaced by DMB. Furthermore, the displacement of the *E*-GSH ligand of E-GSCbl was highly specific for CN^-. Other anions prevalent in environmental media were unreactive, except for S^{2-}, SO_3^{2-} and HSO_3^- (Fig. 6 and supplementary figure). The reaction of *E*-GSCbl with S^{2-}, SO_3^{2-} and HSO_3^- at >50-fold molar equivalents showed generation of unidentified cobalamin derivatives. However the presence of theses anions at 10-fold molar equivalents did not alter lower detection limits of the spectrometric assay and the fluorometric assay (1.0–1.2 μM and 0.02–0.03 μM, respectively). These anion competition assays indicated interference by S^{2-}, SO_3^{2-} and HSO_3^- is likely to be insignificant, although further studies would be required to reveal the effect of S^{2-}, SO_3^{2-} and HSO_3^- on the detection of cyanide.

In the present study, the *E*-GSCbl-based spectrometric assay yielded a lower detection limit of 0.8 μM (21 μg L^{-1}) cyanide (Fig. 7), which was similar to that reported for the corresponding GSCbl-based assay [14]. In addition, we found the *E*-GSCbl-based spectrometric assay had an accuracy of ≥90% for the determination of cyanide in tap water and pond water (Table 1). E-GSH fluorescence was strongly quenched in E-GSCbl, presumably due to intramolecular energy transfer between the fluorophore eosin and the nonfluorescent corrin ring, as was previously demonstrated for profluorescent cobalamin analogs [24]. This quenching of E-GSH fluorescence was immediately reversed by reductive cleavage of a Co—S bond and dissociation of *E*-GSH from E-GSCbl by cyanide (Fig. 5). This profluorescent property of E-GSCbl enabled fluorometric detection of cyanide. The lower detection limit of the fluorometric assay using E-GSCbl was estimated to be 0.01 μM (0.26 μg L^{-1}) (Fig. 8), which was 100-fold more sensitive than the corresponding GSCbl-based assay based on dissociation GSH and conjugation with monochlorobimane (MCB) [14]. This improvement in the detection sensitivity was attributed to the ~40-fold higher intrinsic fluorescence of *E*-GSH as compared with that of the GSH-MCB conjugate under the same conditions. We included 2 h incubation time in the fluorometric assay to complete the generation of CNCbl in the reactions of *E*-GSCbl with cyanide. However simple cyanide detection could be done in 10 min, although the lower detection limit increased to ~0.4 μM (10.4 μg L^{-1}) (supplementary fig. 2). Nanomolar concentrations of cyanide in tap water and pond water were determined with an accuracy of ≥95% using the *E*-GSCbl-based fluorometric assay (Table 1). The strong luminescence of *E*-GSH under UV-light and its quenching in *E*-GSCbl were used to devise a straightforward method for the detection of cyanide by naked-eye. *E*-GSH luminescence was directly proportional to cyanide concentration (Fig. 9). This naked-eye assay had an apparent lower detection limit of 0.1 μM (2.6 μg L^{-1}) for cyanide in water, and this was 200-fold more sensitive than the corresponding GSCbl-based assay.

Considering the extensive use of cyanide in various industries, and the possibility of human exposure to cyanide in fire accidents or the illicit use as poison, the detection of cyanide essentially needs a rapid and sensitive method applicable for field diagnosis. *E*-GSCbl-based methods are highly sensitive and, in particular, the fluorometric assay is one of the most sensitive method to date in our knowledge [9]. Cobalamins are light-sensitive to different extent depending of the axial ligand to the cobalt, which may cause a problem for filed applications of E-GSCbl-based assays. The rate of E-GSCbl photodegradation were determined to be 0.20 μM h^{-1} under room lighting conditions and 0.37 μM h^{-1} under UV exposure (supplementary fig. 3 and 4). These results indicated that E-GSCbl is sufficiently stable within the analysis time for the detection of cyanide. E-GSCbl can be devised in a rapid-portable device format, as previously developed with other cobalamin derivatives [25–27], although further studies are required. Moreover the simple process of E-GSCbl synthesis from commercially available precursors would be an advantage for the application of E-GSCbl-based methods for the detection of cyanide in field diagnosis.

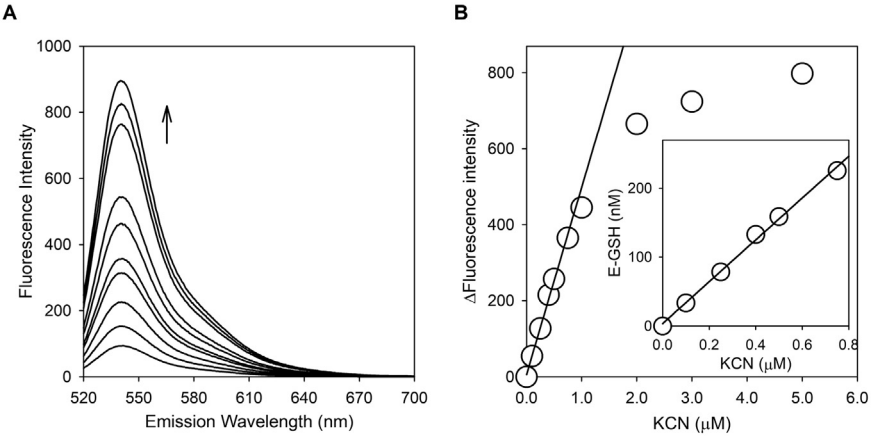

Fig. 8. E-GSCbl-based fluorometric determination of cyanide. (A), fluorescence spectra for the reaction of 1.0 μM E-GSCbl with 0–5.0 μM KCN. The arrow indicates the fluorescence increase at 540 nm by increasing concentrations of cyanide. (B), the plot of ΔF540 nm versus KCN concentration and a simple linear regression analysis (solid lines in inset).

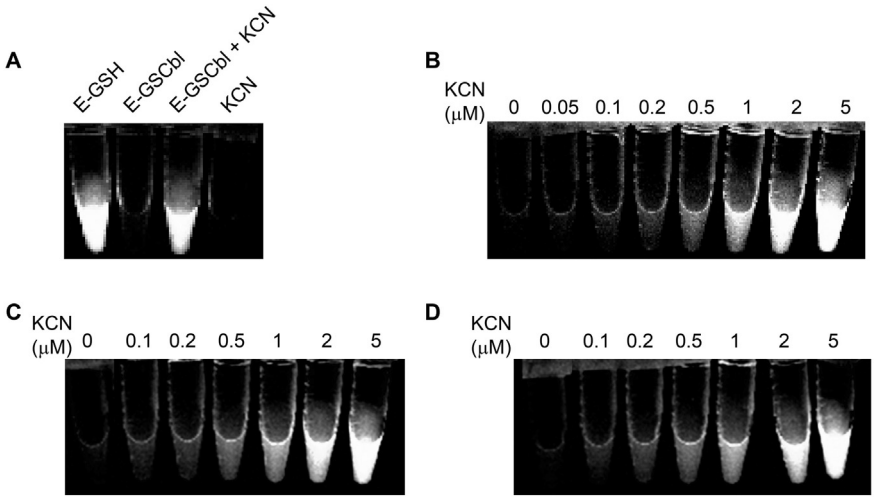

Fig. 9. E-GSCbl-based naked-eye detection of cyanide. Luminance of solutions was detected under UV-light. Solutions in A contained 1.0 μM E-GSH and 1.0 μM E-GSCbl with or without 0.5 mM KCN in deionized H_2O. Solutions contained 1.0 μM E-GSCbl with the indicated concentrations of KCN in deionized H_2O (B), tap water (C) and pond water (D).

5. Conclusions

We developed highly sensitive and straightforward methods for the detection of nanomolar concentrations of cyanide using profluorescent E-GSCbl. The strong fluorescence of E-GSH and its quenching in E-GSCbl was used to detect cyanide. The E-GSCbl-based fluorometric assay yielded a lower detection limit of 0.01 μM (0.26 μg L^{-1}), which, as far as we aware, is lower than claimed for any other method without a complex instrumental system. In addition, the luminance of E-GSH and its quenching in E-GSCbl provide a straightforward naked-eye detection of cyanide at concentrations as low as 0.1 μM (2.6 μg L^{-1}). This study shows E-GSCbl is a novel chemosensor for the detection of trace amounts of cyanide.

Declaration of Competing Interest

There are no conflicts to declare.

Acknowledgements

This research was supported by Yeungnam University research grants in 2017 and 2018.

Appendix A. Supplementary data

Supplementary data to this article can be found online at https://doi.org/10.1016/j.saa.2019.117151.

References

[1] D.M. Beasley, W.I. Glass, Cyanide poisoning: pathophysiology and treatment recommendations, Occup. Med. 48 (1998) 427–431.
[2] K.J. van Buuren, P. Nicholis, B.F. van Gelder, Biochemical and biophysical studies on cytochrome aa 3. VI. Reaction of cyanide with oxidized and reduced enzyme, Biochim. Biophys. Acta 256 (1972) 258–276.
[3] D.A. Dzombak, R.S. Ghosh, G.M. Wong-Chong, Cyanide in Water and Soil: Chemistry, Risk, and Management, CRC/Taylor & Francis, Boca Raton, 2006.
[4] R.M. Gleadow, B.L. Moller, Cyanogenic glycosides: synthesis, physiology, and phenotypic plasticity, Annu. Rev. Plant Biol. 65 (2014) 155–185.
[5] C.J. Knowles, Microorganisms and cyanide, Bacteriol. Rev. 40 (1976) 652–680.
[6] A. Bencini, V. Lippolis, Metal-based optical chemosensors for CN(−) detection, Environ. Sci. Pollut. Res. Int. 23 (2016) 24451–24475.
[7] B.A. Logue, D.M. Hinkens, S.I. Baskin, G.A. Rockwood, The analysis of cyanide and its breakdown products in biological samples, Crit. Rev. Anal. Chem. 40 (2010) 122–147.
[8] J. Ma, P.K. Dasgupta, Recent developments in cyanide detection: a review, Anal. Chim. Acta 673 (2010) 117–125.
[9] R. Jackson, B.A. Logue, A review of rapid and field-portable analytical techniques for the diagnosis of cyanide exposure, Anal. Chim. Acta 960 (2017) 18–39.
[10] F.H. Zelder, Specific colorimetric detection of cyanide triggered by a conformational switch in vitamin B_{12}, Inorg. Chem. 47 (2008) 1264–1266.
[11] F. Zelder, Recent trends in the development of vitamin B12 derivatives for medicinal applications, Chem. Commun. (Camb.) 51 (2015) 14004–14017.
[12] B. Aebli, C. Mannel-Croise, F. Zelder, Controlling binding dynamics of corrin-based chemosensors for cyanide, Inorg. Chem. 53 (2014) 2516–2520.
[13] C. Mannel-Croise, F. Zelder, Side chains of cobalt corrinoids control the sensitivity and selectivity in the colorimetric detection of cyanide, Inorg. Chem. 48 (2009) 1272–1274.
[14] Y. Byun, J. Park, J. Kim, New methods for the detection of cyanide based on displacement of the glutathione ligand of glutathionylcobalamin by cyanide, Int. J. Environ. Anal. Chem. 96 (2016) 845–861.
[15] B. Soto-Blanco, P.C. Marioka, S.L. Gorniak, Effects of long-term low-dose cyanide administration to rats, Ecotoxicol. Environ. Saf. 53 (2002) 37–41.
[16] A. Konstantatos, M. Shiv Kumar, A. Burrell, J. Smith, An unusual presentation of chronic cyanide toxicity from self-prescribed apricot kernel extract, BMJ Case Rep. (2017) 2017.
[17] S.J. Montano, J. Lu, T.N. Gustafsson, A. Holmgren, Activity assays of mammalian thioredoxin and thioredoxin reductase: fluorescent disulfide substrates, mechanisms, and use with tissue samples, Anal. Biochem. 449 (2014) 139–146.
[18] A. Raturi, B. Mutus, Characterization of redox state and reductase activity of protein disulfide isomerase under different redox environments using a sensitive fluorescent assay, Free Radic. Biol. Med. 43 (2007) 62–70.
[19] J. Jeong, J. Park, J. Kim, Processing of glutathionylcobalamin by a bovine B_{12} trafficking chaperone bCblC involved in intracellular B_{12} metabolism, Biochem. Biophys. Res. Commun. 443 (2014) 173–178.
[20] R.K. Suto, N.E. Brasch, O.P. Anderson, R.G. Finke, Synthesis, characterization, solution stability, and X-ray crystal structure of the thiolatocobalamin gamma-glutamylcysteinylcobalamin, a dipeptide analogue of glutathionylcobalamin: insights into the enhanced co-S bond stability of the natural product glutathionylcobalamin, Inorg. Chem. 40 (2001) 2686–2692.
[21] J. Kim, L. Hannibal, C. Gherasim, D.W. Jacobsen, R. Banerjee, A human vitamin B_{12} trafficking protein uses glutathione transferase activity for processing alkylcobalamins, J. Biol. Chem. 284 (2009) 33418–33424.
[22] H.M.N.H. Irving, H. Freiser, T.S. West, Compendium of Analytical Nomenclature: Definitive Rules 1977, 1st ed. Pergamon Press, Oxford; New York, 1978.
[23] L. Hannibal, C.A. Smith, D.W. Jacobsen, The X-ray crystal structure of glutathionylcobalamin revealed, Inorg. Chem. 49 (2010) 9921–9927.
[24] M.S. Rosendahl, G.M. Omann, N.J. Leonard, Synthesis and biological activity of a profluorescent analogue of coenzyme B12, Proc. Natl. Acad. Sci. U. S. A. 79 (1982) 3480–3484.
[25] J. Ma, S. Ohira, S.K. Mishra, M. Puanngam, P.K. Dasgupta, S.B. Mahon, M. Brenner, W. Blackledge, G.R. Boss, Rapid point of care analyzer for the measurement of cyanide in blood, Anal. Chem. 83 (2011) 4319–4324.
[26] J. Ma, P.K. Dasgupta, F.H. Zelder, G.R. Boss, Cobinamide chemistries for photometric cyanide determination. A merging zone liquid core waveguide cyanide analyzer using cyanoaquacobinamide, Anal. Chim. Acta 736 (2012) 78–84.
[27] Y. Tian, P.K. Dasgupta, S.B. Mahon, J. Ma, M. Brenner, J.H. Wang, G.R. Boss, A disposable blood cyanide sensor, Anal. Chim. Acta 768 (2013) 129–135.